

## **Discovery of compounds inhibiting the ADP-ribosyltransferase activity of pertussis toxin**

Yashwanth Ashok<sup>a,#</sup>, Moona Miettinen<sup>b,c,#</sup>, Danilo Kimio Hirabae de Oliveira<sup>a</sup>, Mahlet Z. Tamirat<sup>d</sup>, Katja Näreoja<sup>b</sup>, Avlokita Tiwari<sup>b</sup>, Michael O. Hottiger<sup>e</sup>, Mark S. Johnson<sup>d</sup>, Lari Lehtiö<sup>a,\*</sup> & Arto T. Pulliainen<sup>b,\*</sup>

<sup>a</sup>Faculty of Biochemistry and Molecular Medicine, Biocenter Oulu, University of Oulu, Aapistie 7A, P.O. Box 5400, FI-90014, Oulu, Finland

<sup>b</sup>Institute of Biomedicine, Research Center for Cancer, Infections, and Immunity, University of Turku, Kiinamylynkatu 10, FI-20520, Turku, Finland

<sup>c</sup>Turku Doctoral Programme of Molecular Medicine (TuDMM), University of Turku, Turku, Finland

<sup>d</sup>Structural Bioinformatics Laboratory, Biochemistry, Faculty of Science and Engineering, Åbo Akademi University, Tykistökatu 6A, FI-20520, Turku, Finland

<sup>e</sup>Department of Molecular Mechanisms of Disease, University of Zurich, Winterthurerstrasse 190, 8057, Zurich, Switzerland

# Equal contribution

\* Corresponding authors (Lari.Lehtio@oulu.fi, arto.pulliainen@utu.fi)

**Supporting Information** – Figures S1-S7, Table S1-S2

Figure S1. SEC-analysis of rPtxS1-rGαi complex formation in solution.

Figure S2. Catalytic activity of rPtxS1 is dependent on two acidic amino acids.

Figure S3. rPtxS1 is incapable of ADP-ribosylating a C351A-mutant of rGαi.

Figure S4. Molecular dynamics simulation data.

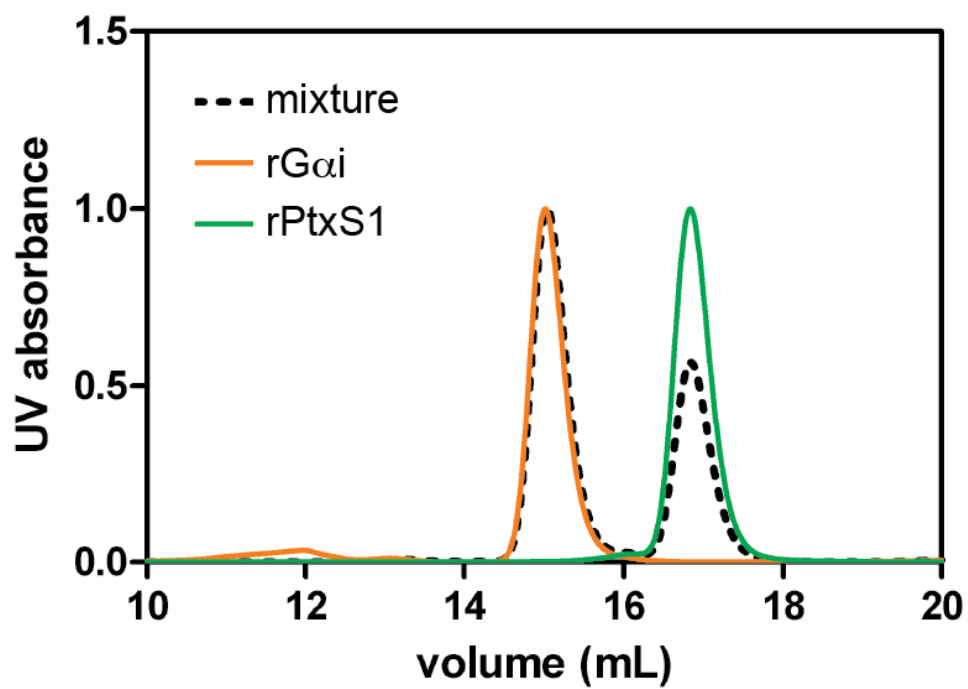
Figure S5. Prediction of binding poses of NSC228155 and NSC29193 to PtxS1.

Figure S6. Effect of NSC228155 on the amount of cell associated PtxS1 and the proteolytic processing of PtxS1.

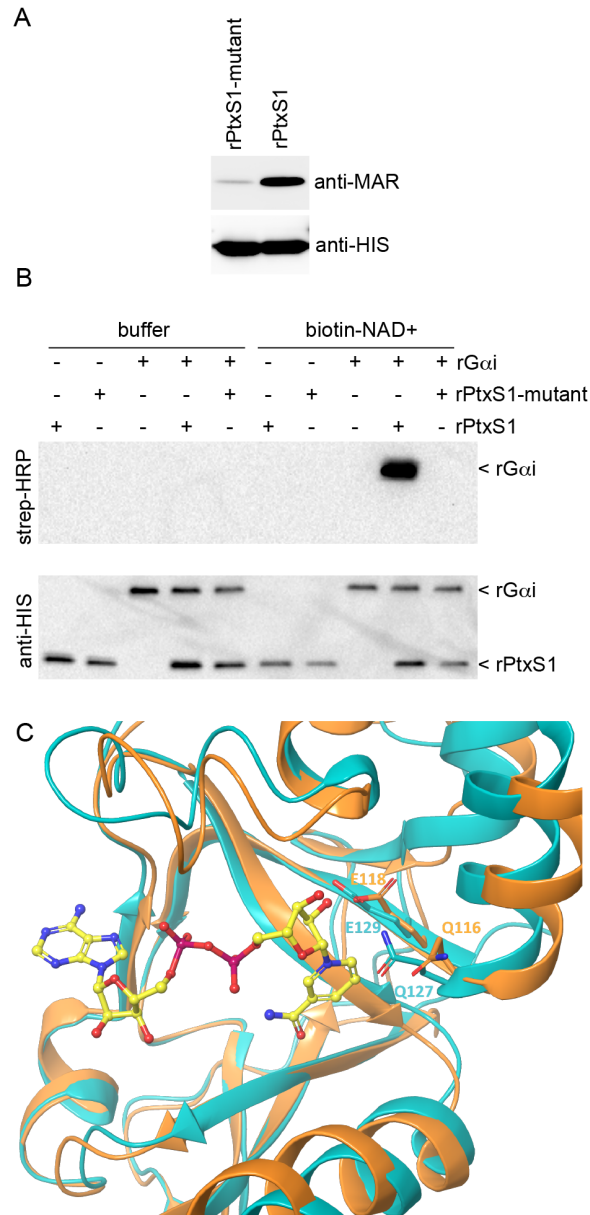
Figure S7. Effect of NSC228155 on the retrograde endosomal trafficking.

Table S1. Assay performance statistic of the *in vitro* NAD<sup>+</sup> consumption assay.

Table S2. ARTD/PARP inhibitory compounds analyzed for rPtxS1 inhibition.



**Figure S1. SEC-analysis of rPtxS1-rGai complex formation in solution.** Proteins were injected into the column either alone (100  $\mu$ g) or in a mixture (100  $\mu$ g + 100  $\mu$ g).



**Figure S2. Catalytic activity of rPtxS1 is dependent on two acidic amino acids.** **A)** Effect of Q127D/E129D mutation to auto-ADP-ribosylation of rPtxS1 that took place inside the *E. coli* expression host. **B)** Effect of Q127D/E129D mutation to rPtxS1-catalyzed ADP-ribosylation of rGαi *in vitro* (substrate-excess conditions). Blots probed, stripped and re-probed in the order of 1) strep-HRP and 2) anti-HIS. **C)** Structural comparison of the NAD<sup>+</sup>-binding pocket of pertussis-like toxin from *E. coli* (PDB\_4Z9C, PDB\_4Z9D) with the corresponding area of PtxS1 (PDB\_1BCP, cyan). NAD<sup>+</sup>-binding pose from Q116/E118 mutant structure of pertussis-like toxin from *E. coli* (PDB\_4Z9D) was superimposed on top of the wild-type structure (PDB\_4Z9C, orange).

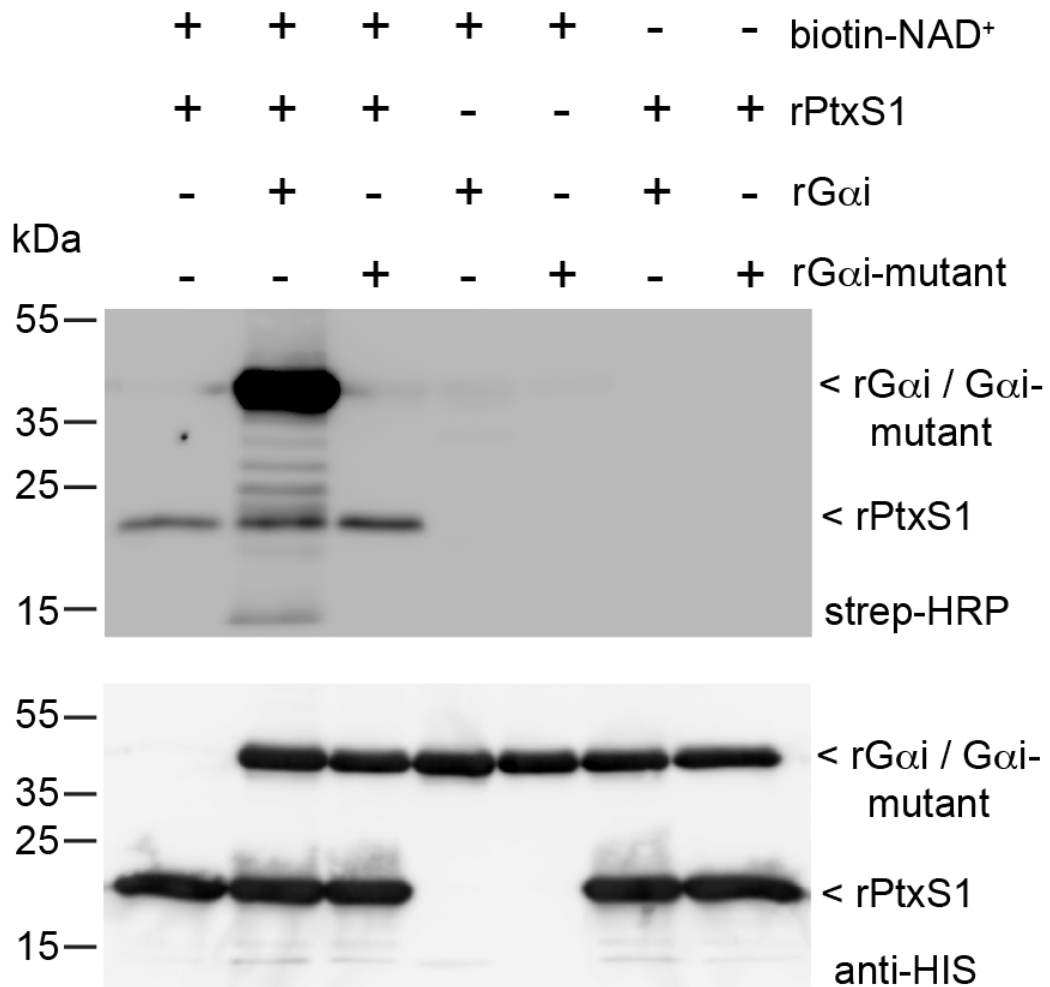


**Figure S3. rPtxS1 is incapable of ADP-ribosylating a C351A-mutant of rG $\alpha$ i.** Effect of C351A mutation to rPtxS1-catalyzed ADP-ribosylation of rG $\alpha$ i *in vitro* (enzyme-excess conditions). Blots probed, stripped and re-probed in the order of 1) strep-HRP and 2) anti-HIS.

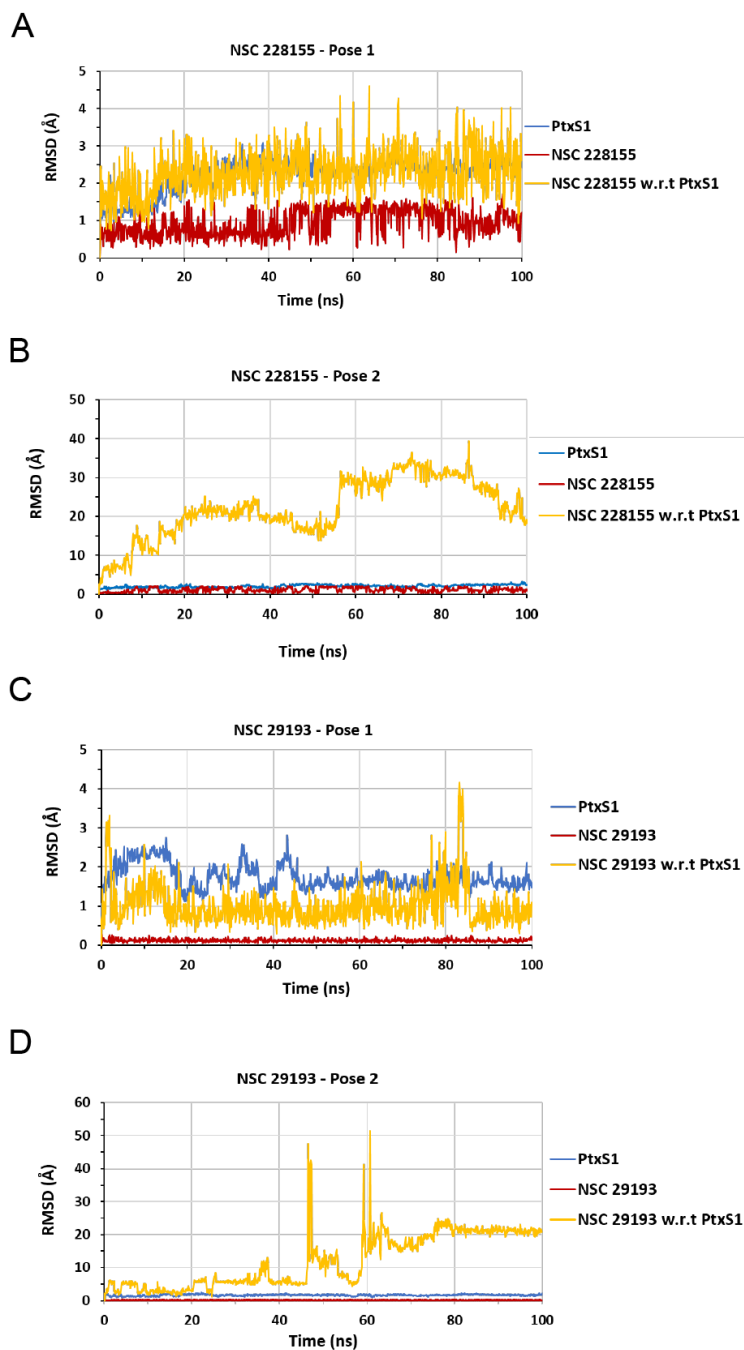


**Figure S4. Molecular dynamics simulation data.** Root mean square deviation (RMSD) of pose 1 **A**) and pose 2 **B**) of NSC228155 and pose 1 **C**) and pose 2 **D**) NSC29193 (see Fig. 5). Backbone atom RMSD of PtxS1 (blue) and the ligands (NSC228155 / NSC29193 - red) based on their first frame structures. Ligand RMSD (yellow) when superimposition is based on pertussis backbone atoms.

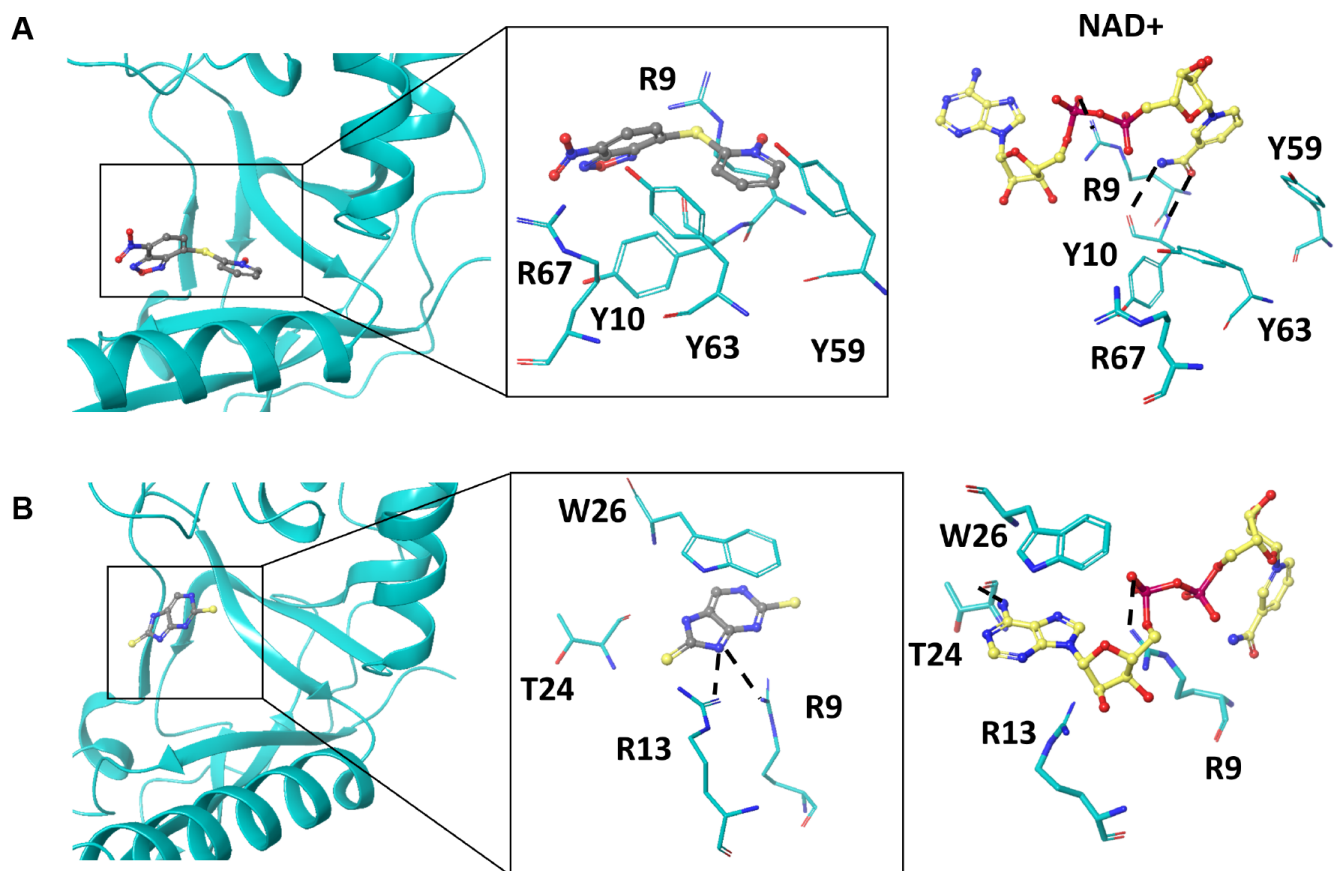


**Figure S5. Prediction of binding poses of NSC228155 and NSC29193 to PtxS1.** Binding pose 2 of NSC228155 (A) and binding pose 2 of NSC29193 (B) to PtxS1 (PDB\_1BCP, chain A). Residues involved in ligand interactions (sticks) and hydrogen bonds (dotted lines) are shown. Binding mode of NAD<sup>+</sup> to PtxS1 in the corresponding area of the NAD<sup>+</sup>-binding pocket is shown in each panel on the right (see also Fig. 1). Color-coding of atoms in NAD<sup>+</sup>: yellow, carbon; blue, nitrogen; red, oxygen; magenta, phosphorus.

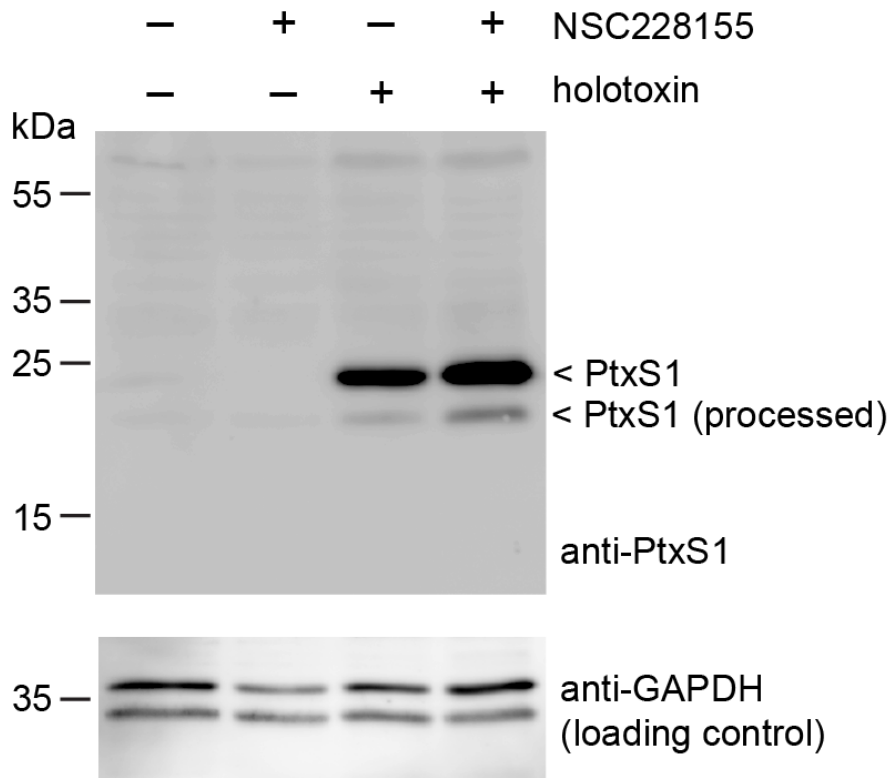


**Figure S6. Effect of NSC228155 on the amount of cell associated PtxS1 and the proteolytic processing of PtxS1.** NSC228155 was added 30 min before starting a 2 h incubation with the pertussis holotoxin (100 ng/mL). Same samples were probed in parallel membranes for PtxS1 and GAPDH.

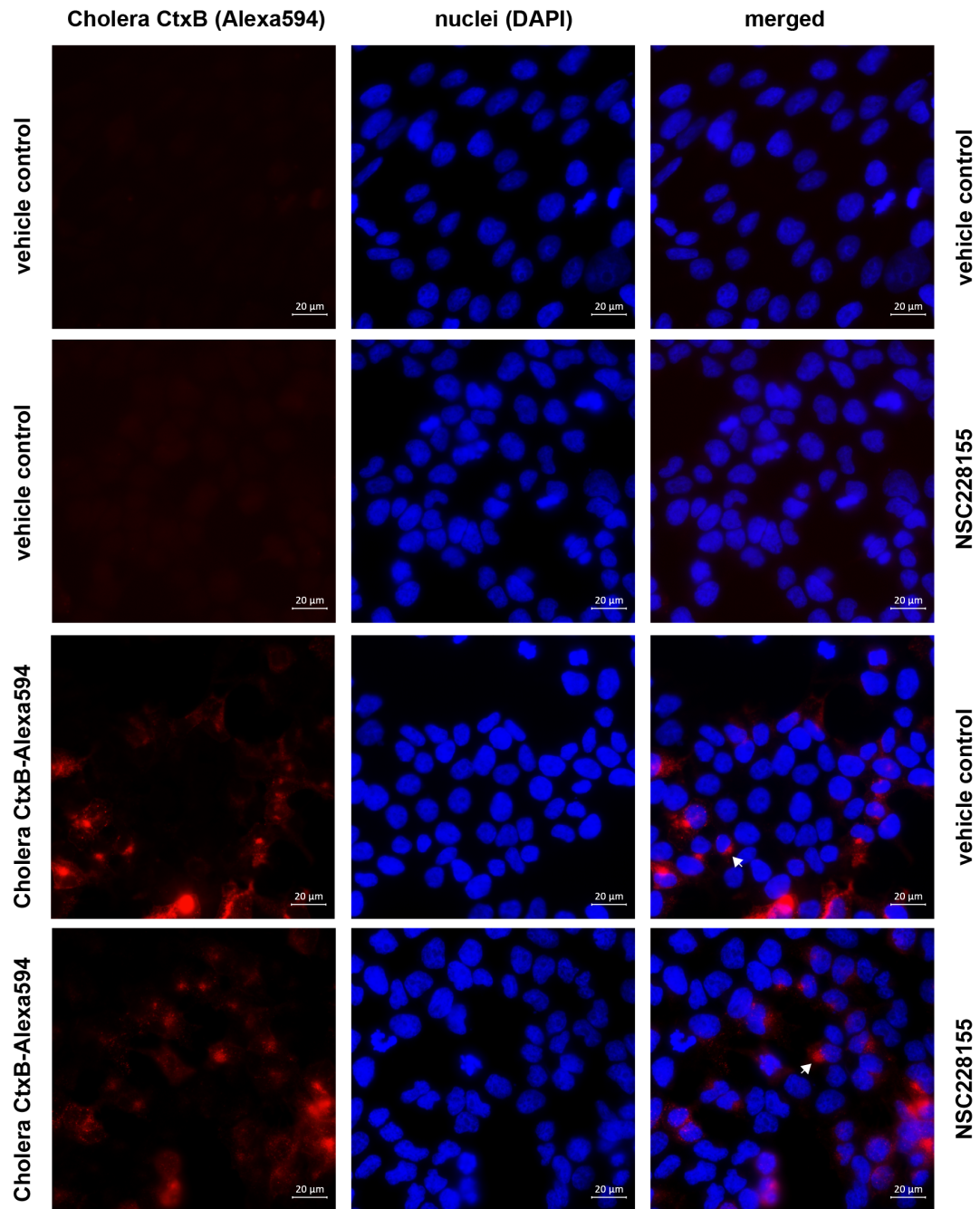


**Figure S7. Effect of NSC228155 on the retrograde endosomal trafficking.** 5  $\mu$ M NSC228155 was added 30 min before starting a 2 h incubation with the retrograde endosomal trafficking marker cholera toxin B subunit conjugated to Alexa594 (1  $\mu$ g/mL). The cells were stained for nuclei with the DNA-binding dye DAPI and imaged with an epifluorescence microscope (40x). Arrows mark examples of the typical accumulations of cholera toxin B subunit close to the nuclei.

**Table S1. Assay performance statistic of the *in vitro* NAD<sup>+</sup> consumption assay.** In order to establish repeatability of values for maximum and minimum signals between plates, wells and days, five control plates were tested. Experimental conditions and protein batches used for assay validation were the same. Three plates were made on one day while second and third days had one plate each.

<b>Parameter</b>	<b>Values</b>
S/B	2.60 ± 0.2
S/N	13.17±1.5
Z'	0.68±0.0
Well-to-well CV% max	3.5±0.9
Well-to-well CV% min	7.8±0.9
Plate-to-plate CV% *	1.2
Day-to-day CV% *	5.6 (5.4 – 5.9) <sup>#</sup>

\*calculated from Z' values

<sup>#</sup>indicates range for Day-to-Day CV

**Table S2. ARTD/PARP inhibitory compounds analyzed for rPtxS1 inhibition.**

Compound name (IUPAC)	Acronym	Supplier
3-aminobenzamide	3-AB	ALEXIS Biochemicals
Nicotinamide		ALEXIS Biochemicals
Benzamide		ALEXIS Biochemicals
2-[(2R)-2-methylpyrrolidin-2-yl]-1H-1,3-benzodiazole-4-carboxamide	Veliparib	Medchemtronica
5-amino-1,2-dihydroisoquinolin-1-one	5-AIQ	ALEXIS Biochemicals
5-amino-3-methyl-1,2-dihydroisoquinolin-1-one	3-Methyl-5-AIQ	ALEXIS Biochemicals
8-amino-3-azatricyclo[7.3.1.0 <sup>5,13</sup> ]trideca-1(12),5,7,9(13),10-pentaene-2,4-dione	4-ANI	ALEXIS Biochemicals
5-[4-(piperidin-1-yl)butoxy]-1,2,3,4-tetrahydroisoquinolin-1-one	DPQ	ALEXIS Biochemicals
2-methyl-1H,4H,5H,7H,8H-thiopyrano[4,3-d]pyrimidin-4-one	DR2313, DRL	ALEXIS Biochemicals
2-(4-{{[(2S,3S,4R,5R)-5-(6-amino-9H-purin-9-yl)-3,4-dihydroxyoxolan-2-yl]carbonyl}piperazin-1-yl)-N-(1-oxo-2,3-dihydro-1H-isoindol-4-yl)acetamide	EB-47	ALEXIS Biochemicals
1,4-dihydroquinazolin-4-one	4-Hydroxyquinazoline	ALEXIS Biochemicals
6-amino-5-iodo-2H-chromen-2-one	INH2BP	ALEXIS Biochemicals
5-hydroxy-1,2-dihydroisoquinolin-1-one	1,5-Isoquinolinediol	ALEXIS Biochemicals
(2E,4S,4aS,5aR,12aS)-2-[amino(hydroxy)methylidene]-4,7-bis(dimethylamino)-10,11,12a-trihydroxy-1,2,3,4,4a,5,5a,6,12,12a-decahydrotetracene-1,3,12-trione	Minocin	ALEXIS Biochemicals
8-hydroxy-2-methyl-1,4-dihydroquinazolin-4-one	NU1025, 4PAX	ALEXIS Biochemicals
5,6-dihydrophenanthridin-6-one	phenanthridone	ALEXIS Biochemicals
2-(dimethylamino)-N-(6-oxo-5,6-dihydrophenanthridin-2-yl)acetamide	PJ-34, P34	ALEXIS Biochemicals
4H,5H-thieno[2,3-c]isoquinolin-5-one	TIQ-A	ALEXIS Biochemicals
1,7-dimethyl-2,3,6,7-tetrahydro-1H-purine-2,6-dione	1,7-dimethylxanthine	Sigma
3-(4-chlorophenyl)quinoxaline-5-carboxamide	CNQ	Calbiochem / WVR
4-({3-[(4-cyclopropanecarbonylpiperazin-1-yl)carbonyl]-4-fluorophenyl}methyl)-1,2-dihydrophthalazin-1-one	Olaparib	Medchemtronica
(4Z)-4-[(1-methyl-1H-pyrrol-2-yl)methylidene]-1,2,3,4-tetrahydroisoquinoline-1,3-dione	BYK204165	Sigma
2-[4-(trifluoromethyl)phenyl]-1H,4H,5H,7H,8H-thiopyrano[4,3-d]pyrimidin-4-one	XAV939	Maybridge
2-(pyridin-2-yl)-5H,7H,8H-thiopyrano[4,3-d]pyrimidin-4-ol	RF03877	Maybridge
2-cyclopropyl-5H,7H,8H-thiopyrano[4,3-d]pyrimidin-4-ol	RF03876	Maybridge
4-[(1R,2S,6R,7S)-3,5-dioxo-4-azatricyclo[5.2.1.0 <sup>2,6</sup> ]dec-8-en-4-yl]-N-(quinolin-8-yl)benzamide	IWR-1	Sigma
N-(6-methyl-1,3-benzothiazol-2-yl)-2-({4-oxo-3-phenyl-3H,4H,6H,7H-thieno[3,2-d]pyrimidin-2-yl}sulfonyl)acetamide	IWP-2	Sigma
4-iodo-3-nitrobenzamide	Iniparib	Selleck Biochemicals
6-fluoro-2-{{4-[(methylamino)methyl]phenyl}-3,10-diazatricyclo[6.4.1.0 <sup>4,13</sup> ]trideca-1,4(13),5,7-tetraen-9-one	Rucaparib, AG014699	Medchemtronica
1-oxo-1,2-dihydroisoquinolin-5-yl benzoate	UPF1035	Enzo Life Sciences
5-(2-oxo-2-phenylethoxy)-1,2-dihydroisoquinolin-1-one	UPF1069	Enzo Life Sciences
2-phenyl-4H-chromen-4-one	Flavone	Sigma